Resonances in the Hartree-Fock BCS theory

A. T. Kruppa
Institute of Nuclear Research of the Hungarian Academy of Sciences, H-4001 Debrecen, Pf. 51, Hungary

P. H. Heenen
Service de Physique Nucléaire Théorique, U.L.B.-C.P.229, B-1050 Brussels, Belgium

R. J. Liotta
Manne Siegbahn Institute of Physics, Frescativagen 24, S-10405 Stockholm, Sweden
(Received 22 November 2000; published 23 March 2001)

Resonance states are introduced into the Hartree-Fock BCS model using a complex scaling method in order to take into account the effect of pair scattering into continuum states. The applicability of the state-dependent BCS model based on bound and resonance states is checked at the proton drip-line region around the double magic nuclei ^{48}Ni by comparing with Hartree-Fock-Bogoliubov calculations.

DOI: 10.1103/PhysRevC.63.044324 PACS number(s): 21.60.Jz, 21.10.Pc, 21.10.Dr, 21.10.Ft

I. INTRODUCTION

Self-consistent mean-field models based on effective interactions are quite succesful in describing a large range of nuclear properties. A key ingredient of such models is the treatment of pairing correlations. For nuclei close to stability, these are usually incorporated with the help of the BCS approximation. However, it has been known since the beginning of the 1980s that the BCS approximation becomes unreliable for nuclei close to drip lines because the coupling between bound and free single-particle states is not correctly treated [1–3]. Too simple a treatment of pairing correlations leads to a sizable probability of the presence of particles outside the nucleus, creating a nonphysical gas.

It was shown [1–3] that a treatment of pairing correlations by the Bogoliubov method always permits one to construct localized normal and pairing densities, provided that the energy of the Fermi level is negative. The quasiparticle wave functions then satisfy either bound-state or scattering-state boundary conditions. The fact that the density matrix vanishes at large distances has the important consequence that states of the canonical basis are also localized, despite the fact that a large fraction of the quasiparticle states is comprised of scattering states. The breakdown of the BCS approximation is due to the fact that the Hartree-Fock (HF) states, which diagonalize the HF Hamiltonian, do not have this property.

Several applications of the Hartree-Fock-Bogoliubov (HFB) theory to nuclei far from stability were performed in the last few years [3–5]. In most cases, the HFB spectrum was discretized by limiting the coordinate space to a box. In applications using finite-range Gogny force, the equations were solved by expanding the individual wave functions on an oscillator basis. However, it was shown in Ref. [3] that the convergence of the continuous part of the spectrum is extremely slow as a function of the size of the basis.

Two main difficulties are related to the use of the Bogoliubov method. As implemented up to now, the continuum is discretized, and quasiparticle states in the continuum do not verify the correct boundary conditions of scattering states. This restriction should not be too difficult to eliminate when a spherical symmetry is imposed on the nuclear density, but it would be hard to remove for deformed nuclei. A second difficulty comes from the fact that even with a discretized continuum, the number of scattering states is huge. Again, the main difficulties arise when all the degeneracies of the single-particle wave functions are removed. However, the continuum of a Hamiltonian is not structureless. The structure of the continuum is reflected in the appearance of resonance states. Narrow resonances are well localized inside the nuclear surface, and they resemble bound states. The difference between bound states and narrow resonances turns up only very far away from the nuclear surface. One may hope that using only resonance states instead of the full continuum, the configuration space will be large enough for the pairing to give good binding energies, even within the BCS approximation. However, this requires some kind of regularization procedure to avoid the spurious effects of a particle gas surrounding the nucleus.

Such a procedure was already developed to avoid spurious effects due to the population of mean-field states in the continuum. In their studies of the statistical properties of hot nuclei, Bonche *et al.* [6,7] also encountered problems of the appearance of a particle gas surrounding the nucleus, but in this case created by temperature effects at the HF level of approximation. Bonche *et al.* introduced a procedure to remove the contribution of unbound nuclear states present in the external nucleon vapor. They also showed that this subtraction procedure leads to nuclear properties independent of the external vapor. An important consequence of this work is that it proves that it is possible to eliminate the spuriousness due to the coupling between bound and continuum states without relying on a Bogoliubov framework.

Appropriately selected scattering states around a resonance were introduced into the BCS theory in Refs. [8,9]. A genuine resonance (Gamow) state, however, is not a scattering state. The Gamow states correspond to poles of the S matrix. These discrete states satisfy a Schrödinger equation with complex energy. One of the aims of this paper is to incorporate Gamow states into the BCS formalism. The use

of Gamow states in BCS theory is not trivial, since the Gamow wave functions are not square integrable. Therefore, a calculation of the corresponding matrix elements requires some type of regularization technique. We will use a complex scaling method, which is actually a general theory to treat resonances [10,11]. Complex scaling was already applied in a self-consistent mean-field model [12,13] but without pairing correlations. Our aim in this paper is to investigate whether one can define a BCS scheme within a well chosen basis which will also enable one to incorporate the behavior of resonant states correctly.

We will apply the BCS formalism with resonances to the proton-rich $N=20$ and 22 isotones. The structure of these nuclei has been investigated within the HFB framework in Ref. [4]. It is expected that the BCS formalism performs better in the proton drip-line region than in the case of neutron drip line nuclei [4,14] but that it can accurately give only relative binding energies, i.e., separation energies [4]. In this paper we show that the extended BCS theory, which uses only a few resonances instead of the full continuum, often gives absolute binding energies in very good agreement with the HFB description. At the same time we obtain correct values for the nuclear radii, and the ''particle-gas'' problem is partly avoided.

The paper is organized as follows. In Sec. II, the bound, scattering, and resonance states of the HF mean field are introduced. The resonance states are included in the BCS formalism in Sec. III. In Sec. IV, the resonances of the nuclei ^{40}Ca and ^{48}Ni are calculated in the HF model. The proton drip-line nuclei with neutron numbers 20 and 22 and charge numbers 22, 24, and 26 are considered in the BCS theory, with resonances, in Sec. V. The conclusion is given in Sec. VI.

II. BOUND, SCATTERING, AND RESONANCE STATES IN HF MEAN FIELD

The standard HF approximation is valid only for bound nuclei. The mean-field potential is then determined by bound orbits. However, the spectrum of the HF Hamiltonian contains not only bound states but also scattering and resonances states. In this section we present definitions concerning these unbound states.

For Skyrme-type interactions, the Hartree-Fock equation, assuming spherical and time-reversal symmetry, is of the form [2]

$$\hat{h}u(r)=eu(r), \tag{1}$$

where the HF operator reads

$$\hat{h}=-\frac{d}{dr}M(r)\frac{d}{dr}+M(r)\frac{l(l+1)}{r^2}+V(r)+V_{so}^{lj}(r)+\frac{dM}{dr}\frac{1}{r}. \tag{2}$$

The r-dependent form factors—the particle-hole inertia parameter $M(r)$, central potential $V(r)$ and spin-orbit term $V_{so}^{lj}(r)$—are expressed by the functionals of the occupied single-particle orbits [2],

$$\chi_\alpha(\mathbf{r})=\frac{u_{nlj}(r)}{r}[Y_l\chi_{1/2}]^{jm}, \tag{3}$$

where $[\cdots]^{jm}$ stands for the angular momentum coupling of the orbital and spin angular momenta, and α denotes the quantum numbers n, l, j, and m. Operator (2) contains first- and second-order derivatives.

Using the transformation

$$u(r)=f(r)/M(r)^{1/2}, \tag{4}$$

we obtain the second-order differential equation

$$-\frac{d^2f}{dr^2}+\frac{l(l+1)}{r^2}f(r)+\frac{V(r)+V_{so}^{lj}(r)+V_M(r)}{M(r)}f(r)=e\frac{1}{M(r)}f(r), \tag{5}$$

where a new ''potential'' term occurs:

$$V_M(r)=\frac{M''}{2}-\frac{M'^2}{4M}+\frac{M'}{M}. \tag{6}$$

In order to obtain a unique solution of Eq. (5), one must supply two boundary conditions. The first is the regularity requirement at the origin:

$$f_\alpha(0)=0. \tag{7}$$

For large r the particle-hole inertia parameter $M(r)$ tends to $\hbar^2/(2m)$, where m is the nucleon mass, so Eq. (5) looks like a radial Schrödinger equation. The second boundary condition is then the outgoing wave,

$$f'_\alpha(R)/f_\alpha(R)=k_\alpha O'_l(k_\alpha R)/O_l(k_\alpha R), \tag{8}$$

at a distance R where the potential terms of Eq. (5) can be considered to be zero. In Eq. (8), $O_l(\rho)=G_l(\rho)+iF_l(\rho)$ is the outgoing-wave Coulomb wave function. The wave number is given by $k_\alpha=(2me_\alpha/\hbar^2)^{1/2}$. Purely imaginary wave numbers $k_\alpha=i\kappa_\alpha$ ($\kappa_\alpha>0$) correspond to a bound state with energy $e_\alpha=-\hbar^2\kappa_\alpha^2/2m$. Once the self-consistent HF mean-field potential has been determined, its continuous spectrum and the resonances can be calculated by replacing boundary condition (8) with a new one.

The self-consistent mean field supports scattering states which are solutions of Eq. (5), with the following set of boundary conditions:

$$f_{l,j}^E(0)=0 \tag{9}$$

and

$$f_{l,j}^E(R)=\tfrac{1}{2}i\exp[i\sigma_l(E)][O_l(kR)^*-S_{l,j}(E)O_l(kR)]. \tag{10}$$

Here E is an arbitrary positive real number, the wave number is $k=(2mE/\hbar^2)^{1/2}$, and $\sigma_l(E)$ is the Coulomb phase shift. The scattering S matrix can be expressed by the phase shift

$\delta_{l,j}(E)$ as $S_{l,j}(E)=\exp[2i\delta_{l,j}(E)]$. In analogy with the bound states, we can define the scattering solutions

$$\chi_{Eljm}(\mathbf{r})=\frac{f^E_{lj}(r)}{r}[Y_l\chi_{1/2}]^{jm}. \tag{11}$$

The bound and scattering states form a basis on which any state can be decomposed. We shall call this the standard basis.

The poles of the scattering matrix on the complex energy plane (which is a Riemann surface with two sheets) are very important. Their positions correspond to the energies of the bound and resonance states. These latter have complex energies $w_\alpha=e_\alpha-i\Gamma_\alpha/2$, whose imaginary part determine the half-life-time of the state $T_{1/2}=\ln(2)\hbar/\Gamma_\alpha$.

The resonance or Gamow states satisfy boundary conditions similar to the bound states [see Eqs. (7) and (8)], but with a complex wave number $k_\alpha=\kappa_\alpha-i\gamma_\alpha$ $(\kappa_\alpha,\gamma_\alpha>0)$. The relationship between the energy and the wave number is also unchanged: $w_\alpha=\hbar^2k^2_\alpha/2m$. Gamow states represent decaying systems. They do not belong to the Hilbert space of the physical system, and are not normalizable in the usual sense. Different but equivalent methods have been introduced to normalize them in a generalized sense [15]. For our purposes we will use another property of Gamow states. The resonances, together with bound states and with suitably defined scattering states with complex energy, form a complete set of states [16] which is sometimes called the Berggren basis [17].

III. RESONANCES IN HF-BCS THEORY

In this section, a brief reminder of the HFB theory is presented first, and then the resonance states are introduced into the HF-BCS theory. In coordinate space the HFB equations are

$$\begin{pmatrix}\hat h-\lambda & \hat\Delta\\ \hat\Delta & \lambda-\hat h\end{pmatrix}\begin{pmatrix}\phi^{(1)}_\alpha(\mathbf{r})\\ \phi^{(2)}_\alpha(\mathbf{r})\end{pmatrix}=E_\alpha\begin{pmatrix}\phi^{(1)}_\alpha(\mathbf{r})\\ \phi^{(2)}_\alpha(\mathbf{r})\end{pmatrix}, \tag{12}$$

where λ is the Fermi energy and E_α is the quasiparticle energy. For simplicity the spin degree of freedom is omitted. The operators $\hat h$ and $\hat\Delta$ are the mean-field particle-hole and particle-particle Hamiltonians, respectively [2,3]. Generally $\hat h$ and $\hat\Delta$ are integral operators. They are complicated functionals of $\phi^{(1)}$ and $\phi^{(2)}$. Assuming time-reversal invariance, spherical symmetry and a Skyrme-type effective interaction $\hat h$ are given by Eq. (2).

The quasiparticle wave functions $\phi^{(1)}$ and $\phi^{(2)}$ can be expanded on any basis to transform the coordinate space HFB equation (12) in matrix form [18]:

$$\begin{pmatrix}h-\lambda & \Delta\\ \Delta & \lambda-h\end{pmatrix}\begin{pmatrix}U_\alpha\\ V_\alpha\end{pmatrix}=E_\alpha\begin{pmatrix}U_\alpha\\ V_\alpha\end{pmatrix}. \tag{13}$$

The matrix h corresponds to the HF mean field,

$$h_{ij}=t_{ij}+\sum_{kl}(V_{ikjl}+V_{i\bar k j\bar l})\rho_{kl}, \tag{14}$$

and the pairing gap matrix reads

$$\Delta_{ij}=\sum_{kl}V_{ij\bar k\bar l}\kappa_{\bar k\bar l}. \tag{15}$$

In these expressions ρ_{ik} and κ_{ik} are the matrix elements of the one-body density matrix ρ and the pairing tensor κ, respectively. For a given basis state i the time-reversed state is denoted by $\bar i$. From the solution vectors U_α and V_α the matrices U and V can be composed, and the density and pairing matrices can be written as $\rho=VV^+$ and $\kappa=UV^+$.

The HFB equation (12) is nonlinear, and is solved by iterations. At any iteration step, approximations of the operators $\hat h$ and $\hat\Delta$ are constructed from the wave functions of the previous iteration. To write Eq. (12) in the form of Eq. (13), we will follow the two-bases method described in Refs. [5,19], in which the eigenfunctions of Eq. (12) are expanded on the complete set of eigenfunctions of the HF operator $\hat h$. This basis is composed of the bound and scattering states of $\hat h$, i.e.,

$$\text{standard basis}=\{\chi_\alpha,\chi_{Eljm}|E\in(0,\infty)\ \text{ and }\ \alpha\in\text{bound states}\}. \tag{16}$$

The scattering states are usually discretized using box boundary conditions [2,3]. The index i in Eqs. (14) and (15) refers either to a bound state or to a discretized continuum state. Since the HF basis is used, the matrix (14) can be simplified, $h_{ij}=\delta_{ij}e_i$, where δ_{ij} is the Kronecker δ and e_i is the energy of a bound or a discretized continuum state. Basis (16) is the standard complete system of the HF operator $\hat h$.

Within the Berggren basis the continuum part of a self-adjoint Hamiltonian is replaced by resonance states and suitably chosen scattering states with complex energy. This basis is also complete [16], and is composed of

$$\text{Berggren basis}=\{\chi_\alpha,\chi_{zljm}|z\in L^+\ \text{ and }\ \alpha\in\text{bound and resonance states}\}, \tag{17}$$

where L^+ is a properly chosen path in the complex k plane [16,17]. The Berggren basis was already used in nuclear structure calculations, for example in the resonance random-phase approximation developed in Ref. [20] and in the multistep shell model of Ref. [21]. The properties of the Berggren basis were thoroughly investigated in the literature [22].

The continuum part of the Berggren basis, corresponding to the complex path L^+, can be discretized. The HFB equations in the Berggren basis are similar to Eqs. (13)–(15), with indices i and j belonging to Eq. (17).

We shall now introduce two approximations to solve the HFB equations. First, the complex continuum will be neglected. The validity of this approximation in some nuclear models was investigated in Refs. [23,24], with the conclusion that the nonresonant background continuum can be

safely neglected. This means that the resonance part of the Berggren basis takes care of a large portion of the continuum part of the standard basis. However, the observables will become complex numbers in this approximation. The magnitude of their imaginary parts gives a measure of the validity of this approach.

In order to further simplify the solution of the HFB equation, we make a state-dependent BCS approximation. That is, the off-diagonal part of the pairing matrix is neglected. In this way the solution of Eq. (12) acquires the forms

$$\phi_i^{(1)} = u_\alpha \chi_i \quad \text{and} \quad \phi_i^{(2)} = v_i \chi_i . \tag{18}$$

Here the index i refers to the bound and resonance solutions of $\hat{h}$, and u_i and v_i are the usual BCS parameters. Having solved Eq. (12), at a given iteration we recalculate the densities and generate new particle-hole and particle-particle Hamiltonians $\hat{h}$ and $\hat{\Delta}$. The bound and resonance states of this new HF operator constitute the basis of the next iteration step. This procedure is repeated until convergence is achieved. We will call this method the self-consistent HF-BCS model with resonances (HF-BCS-R). In Ref. [1] the effect of the quasiparticle continuum of the HFB equation and its relation to the BCS approach was investigated thoroughly. However in the model of Ref. [1] the HF Hamiltonian was kept fixed during the iteration.

Because the resonance wave functions are not localized, the potentials of $\hat{h}$ and $\hat{\Delta}$ do not tend to zero for large r. To overcome this difficulty we carry out a complex scaling from the very beginning of the calculation. The complex scaled operator $\hat{h}_\Theta = \hat{U}_\Theta \hat{h} \hat{U}_\Theta^{-1}$ is taken in Eq. (12) instead of $\hat{h}$. The nonunitary scaling operator is defined by $(\hat{U}_\Theta f)(\mathbf{r}) = f[\exp(i\Theta)\mathbf{r}]$, where $f(\mathbf{r})$ is an arbitrary wave function.

The calculation of the pairing gap matrix in the BCS approach with contact interaction in the particle-particle channel requires the evaluation of the following integral:

$$\int_o^\infty \frac{1}{r^2} u_\alpha^2(r) u_{\alpha'}(r)^2 \, dr. \tag{19}$$

If one of the wave functions in the above integrand is a resonance state, the integral is divergent. It is made convergent by calculating the integral along the complex ray $r\exp(i\Theta)$. The result is independent of the value of the complex scaling parameter Θ. This type of technique was used, for example, in Ref. [20].

A BCS model with resonances was introduced in Refs. [8,9]. In these works, the standard basis was used instead of the Berggren basis. The continuum states were considered around a resonance, and the corresponding scattering solutions weighted to take into account the effect of the width. In contrast, in our approach we follow the procedure of Refs. [17,21–24]. The standard basis is replaced by the Berggren one, and the effect of the Gamow states is investigated.

Integral (19), which in principle diverges for Gamow as well as scattering states, is made convergent in Ref. [9] by restricting the upper limit of the integration to a finite value. The complex scaling, on the other hand, is a well-established method to regularize integral (19). Within this method the resulting integral does not depend upon any cutoff parameter. In particular, it can be shown that the value of the integral is in general independent upon the complex scaling parameter.

TABLE I. The position and width of the single-particle proton resonance states of the nucleus ^{48}Ni with Skyrme force Sly4 obtained with the HF approximation. The results correspond either to the poles of the S matrix (Gamow state) or to the phase-shift definitions of the energies and widths

	Gamow		Phase shift	
State	e_α (MeV)	Γ_α (MeV)	e_α (MeV)	Γ_α (MeV)
$2p_{3/2}$	2.856	0.0132	2.856	0.0132
$2p_{1/2}$	4.288	0.168	4.288	0.171
$1f_{5/2}$	6.811	0.113	6.811	0.114
$1g_{9/2}$	10.266	0.255	10.266	0.256

IV. RESONANCE STATES IN THE HF MEAN FIELD

For the numerical integration of differential equation (5), we have used the Fox-Goodwin method. The eigenvalue problem is solved using a generalization of the method described in Ref. [25]. For the effective nucleon-nucleon interaction we have selected the Skyrme force Sly4 [26]. The HF equation is solved by an iteration technique. The starting single-particle orbits are generated using an appropriately chosen Woods-Saxon potential.

We have investigated the resonance states of two nuclei within the HF approximation: a stable one, ^{40}Ca, and its isotone at the proton drip line, ^{48}Ni. The real and imaginary parts of the energy of the proton resonance states are shown in Tables I and II. The only resonances below the Coulomb barrier are the first two. Since the Coulomb barrier is not very high, the widths of the states are not very narrow.

In Fig. 1, the wave functions of the $2p_{3/2}$ proton orbit are displayed for both ^{48}Ni and ^{40}Ca. They are very similar up to $r=10$ fm, which corresponds to the position of the Coulomb barrier. Beyond this point, the characteristic oscillatory behavior of the Gamow states appear very clearly only for ^{48}Ni, in which case the imaginary part becomes significant at $r=15$ fm. This difference in behavior between both nuclei is related to the different widths of the state $2p_{3/2}$.

As explained above, for the resonance wave functions we use the transformation $r \to r\exp(i\Theta)$. The wave function $u_\alpha[r\exp(i\Theta)]$ is the solution of the complex scaled HF equa-

TABLE II. As in Table I, for the nucleus ^{40}Ca.

	Gamow		Phase shift	
State	e_α (MeV)	Γ_α (MeV)	e_α (MeV)	Γ_α (MeV)
$2p_{3/2}$	1.111	0.000162	1.111	0.000172
$2p_{1/2}$	2.755	0.0931	2.755	0.0940
$1f_{5/2}$	4.820	0.0570	4.820	0.0572
$1g_{9/2}$	8.423	0.176	8.423	0.177

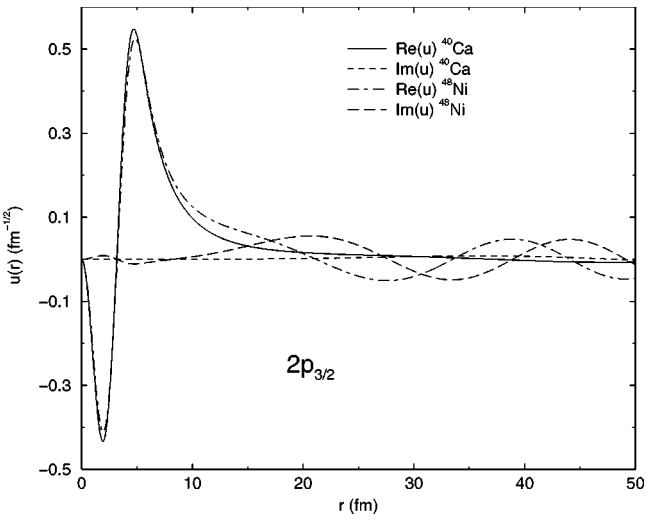

FIG. 1. The wave function of the $2p_{3/2}$ proton resonance orbit in ^{48}Ni and ^{40}Ca using the Skyrme force Sly4 and the HF model.

tion [12]. In Fig. 2 the wave function of the $2p_{3/2}$ orbit of the nucleus ^{48}Ni is displayed for $\Theta=0$ (original Gamow state) and for $\Theta=0.1$ rad. The amplitude of the oscillation of the wave function is damped when complex scaling is applied. The square integrability of the resonance wave function along the complex ray $r\exp(i\Theta)$ is essential in the calculation of the pairing matrix.

The position and width of a resonance can also be determined by the behavior of the phase shifts. We have solved the differential equation (5) using the boundary conditions given by Eqs. (9) and (10). In Fig. 3 the phase shifts are displayed for ^{48}Ni, and for the partial waves $p_{3/2}$, $p_{1/2}$, $f_{5/2}$, and $g_{9/2}$. At the position of the resonance, the phase shift increases rapidly with a slope, depending on the width of the resonance. The position is determined by the energy at which the phase shift presents an inflection point. Its width can be

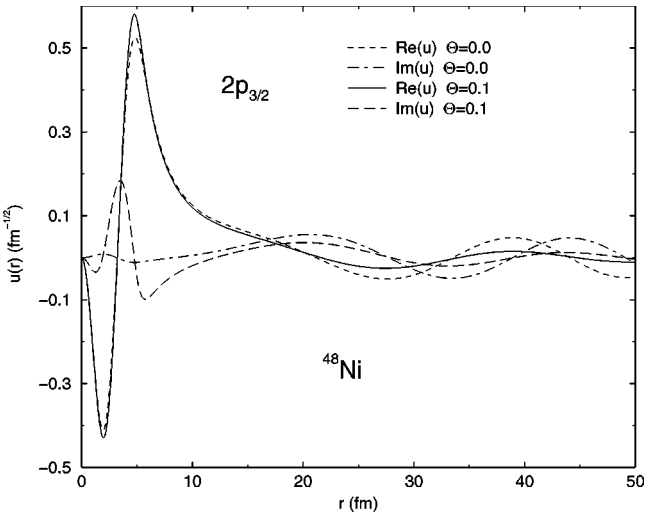

FIG. 2. The wave function of the $2p_{3/2}$ proton resonance orbit in ^{48}Ni using the Skyrme force Sly4 and the HF model. The original Gamow state ($\Theta=0.0$) and the complex scaled wave function ($\Theta=0.1$) are displayed.

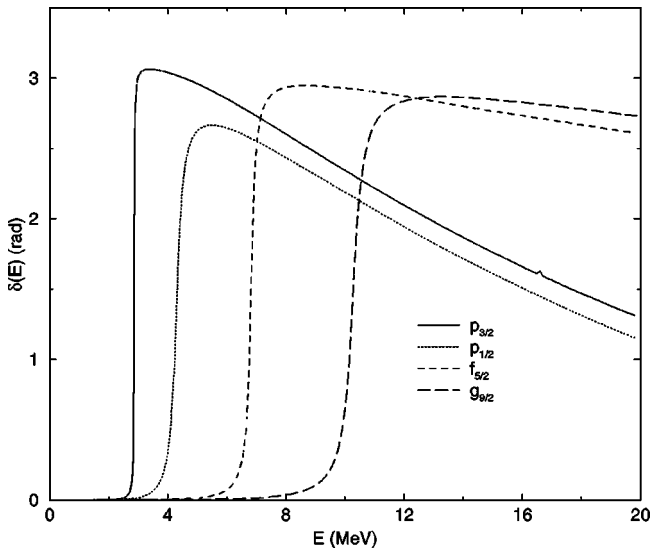

FIG. 3. Partial-wave phase shifts for the nucleus ^{48}Ni using the Skyrme force Sly4 and the HF model.

calculated by the formula $\Gamma=2[d\delta_{l,j}(E)/dE]^{-1}$, where the derivative of the phase shift with respect to the energy is taken at the position of the resonance. These definitions follow from the *R*-matrix theory, with the assumption that the background phase shift can be neglected, and that the one-level *R*-matrix expression is valid. The definitions of a resonance due to the pole of the *S* matrix and to an analysis of the phase shifts should agree only for narrow resonances. In Tables I and II we present the positions and widths of the states determined by both methods. The agreement between the two calculations is excellent. We emphasize that the *S*-matrix definition is unique, whereas the phase-shift definition depends on the assumption that the background phase shift is negligible.

V. BCS CALCULATIONS WITH RESONANCES

The weakly bound drip-line nuclei are most sensitive to coupling by pairing correlations between bound and continuum states. This is the region where the effects of the breakdown of the BCS approximation should be the largest [1,14,27]. In this section, we focus on the proton drip-line nuclei for $20\leqslant Z\leqslant 28$. A restriction to spherical shapes for the proton-rich nuclei with $N=18$, 20, and 22 is well justified [28,29]. The calculations are performed with the Skyrme parametrization Sly4$^{\delta\rho}$. The mean-field interaction Sly4 [26] is supplemented by a density-dependent surface-pairing interaction [27] in the pairing channel,

$$V_P=\left(V_0+\frac{1}{6}V_3\rho(\mathbf{r}_1)^\gamma\right)\delta(\mathbf{r}_1-\mathbf{r}_2) \tag{20}$$

with $V_0=2488.91$ MeV fm^3, $V_3=19990$ MeV fm^3, and $\gamma=1/6$.

We shall compare our results obtained with the HF-BCS-R approximation to spherical HFB calculations [30]. Before doing this, to be able to compare absolute energies, one must check the numerical accuracy of the different com-

TABLE III. The binding energy (E), root mean square radius (r^2), and Fermi level (λ) in different self-consistent mean-field models for the $N=20$ isotones.

	^{42}Ti			^{44}Cr			^{46}Fe		
	$-E$	r^2	$-\lambda$	$-E$	r^2	$-\lambda$	$-E$	r^2	$-\lambda$
HFB	350.84	3.50	2.88	354.39	3.58	1.49	355.51	3.65	0.33
HF-BCS-B	350.52	3.50	2.84	353.95	3.57	1.59	355.15	3.64	0.54
HF-BCS-R1	350.65	3.51	2.89	354.13	3.58	1.61	355.28	3.64	0.51
HF-BCS-R2	350.90	3.51	2.98	354.44	3.58	1.63	355.51	3.65	0.45

puter codes in cases where there are comparable. For the doubly magic nuclei ^{48}Ni and ^{40}Ca, the HF energies that we obtain are -354.49 and -344.26 MeV, respectively whereas the calculation of Ref. [30] gives -354.46 and -344.25 MeV. The agreement between the two calculations is excellent. This implies that in the comparisons done below, discrepancies larger than 100 keV will be due to reasons of physical relevance and not to the numerical procedures.

The total binding energies in the HFB, HF-BCS-R, and HF-BCS-B calculations are given in Table III. The proton Fermi level and the root-mean-square charge radii are also shown. In the case labeled by HF-BCS-B, only bound state orbits are used in the BCS calculation. In the HF-BCS-R1 calculations, with $N=20$ (Table III), only the $2p_{3/2}$ resonance is included, whereas in the HF-BCS-R2 calculation both the $2p_{3/2}$ and $1f_{5/2}$ resonance states are used. The HFB calculations [30] have been carried out using a box with a 20-fm mesh size, and a step length for the numerical integration of 0.25 fm. The pairing phase space has been restricted to $j\leqslant 9/2$. The HFB results do not change if the phase space is cut off at $j\leqslant 19/2$. However, the HFB results do change by at least 1 MeV if all quasiparticle states up to the height of the barrier in a given j and l are taken into account.

It is clear from Table III that including only bound orbits in the BCS theory leads to too small a space. The binding energy in the HF-BCS-B case deviates from the HFB result by 0.5 MeV. However, the BCS scheme, including the two narrowest proton resonance states, agrees very well with the HFB result. The root-mean-square radius of the HF-BCS-R models in Table III shows no sign of the ''particle-gas'' problem.

Since we are using resonance states and neglecting the complex continuum part of the Berggren basis, all physical quantities contain an imaginary part. It is only when the contributions of the complex continuum to the resonance part are included that all physical quantities are given by real numbers. This compensation was observed, e.g., in Ref. [31] where the Berggren basis was introduced in a different nuclear model. The imaginary parts of the quantities listed in Table III are small. The binding energy has an imaginary part of around 5 keV in the HF-BCS-R1 calculation. Adding one more resonance, in the HF-BCS-R2 calculation, the imaginary part of the binding energy is increased to 100 keV. The imaginary parts of the root-mean-square radius are 0.0007 and 0.01 fm in the HF-BCS-R1 and HF-BCS-R2 calculations, respectively.

The proton density, close to the proton drip line, is a key quantity which enables one to put into evidence the presence of a gas external to the nucleus. Its form in the HF-BCS approach is given by

$$\rho(\mathbf{r})=\sum_i v_i^2|\chi_i(\mathbf{r})|^2. \tag{21}$$

Since we used the complex scaling method, the densities are obtained on the complex ray $r\exp(i\Theta)$. In order to obtain the physical densities, we have to rotate the single-particle wave functions back onto the real axis. This is done numerically using the fact that the complex scaling operator acting on the radial wave functions can be written as $\hat{U}(\theta)=\exp[i\Theta r(\partial/\partial r)]$. We have performed a Taylor expansion of the exponential, and truncated it to the fourth order.

It is difficult to distinguish between the resonant and nonresonant continua if the standard basis is used. If all the discretized states are introduced in a BCS calculation, then the nonlocalized continuum states contribute significantly to the matter density, leading to a particle gas. This unphysical property is in principle also present in our HF-BCS-R approach: the resonance wave functions are not localized, and produce nonvanishing densities far away from the nucleus. However, if only a few narrow resonance states are used, one can expect that they do not contribute to the matter density in any physically meaningful region.

To look at this problem quantitatively, we display the proton density for the nucleus ^{46}Fe in Fig. 4. The energy of its Fermi level is -0.45 MeV, and it is expected that the isotone closest to the drip line is where proton pairing correlations will be significant. Figure 4 shows the magnitude of the real part of the density. The imaginary part is smaller than 10^{-4} fm^{-3} everywhere. The density exhibits an oscillatory behavior for very large r. This is inherited from the resonance states taking part in the Berggren basis. For the HF-BCS-R2 calculation the contribution of the density of the $2p_{3/2}$ and $1f_{5/2}$ resonance orbits is also plotted. Beyond 12 fm the total density is determined solely by the resonances. Below this radius, the contribution of these resonances is small, and does not significantly affect the density.

An interesting feature of our calculation is that the values of the mean-square radii are reasonable. This may be surprising considering the unphysical oscillatory pattern of the density at large r, or, more importantly, considering that the Gamow wave functions are not localized and diverge at infinity. However, due to the definition of the inner product in the Berggren representation, the matrix elements of observables, such as the root-mean-square radius, converge. This

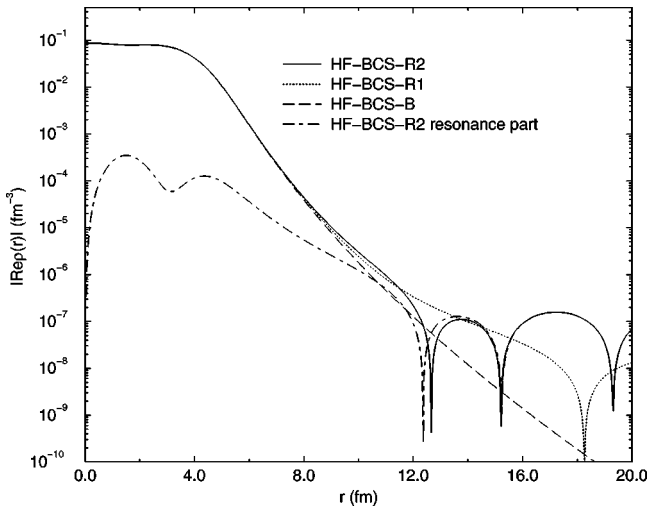

FIG. 4. Magnitude of the real part of the proton density of the nucleus ^{46}Fe obtained using the Skyrme force Sly4 and the BCS approximation including different number of resonant states. In the case of HF-BCS-R2, the resonance contribution to the total density is shown by a dot-dashed line.

feature supports the use of the Berggren basis, as already pointed out in Ref. [32] where the definition of the root-mean-square radius was studied for resonance states.

Up to now, we have looked to $N=20$ nuclei with $20 \leqslant Z \leqslant 28$. Due to the $N=20$ shell closure, neutron pairing correlations can be neglected. This is no longer true for the $N=22$ nuclei. In order to determine which are the relevant resonance neutron orbits, we have calculated the neutron resonances in the HF mean field of ^{48}Ni. The results are shown in Table IV. Since the HF-BCS-R calculation is meaningful only for narrow resonance states, we will use only one resonance neutron orbit, the state $1g_{7/2}$, and the same orbits for the protons as for the $N=20$ isotones. Interestingly, during the iterative solution of the HF-BCS-R equations, the energies of the four proton orbits given in Tables I and II for ^{48}Ni for the HF model decrease, and their widths become lower than 100 keV. We then performed several calculations including resonances of increasing widths. Thus, in Table V, HF-BCS-Rn means that the n narrowest single-particle resonances are taken into account in the BCS procedure.

From this table we can draw the same conclusions as for the $N=20$ isotones. The BCS calculation with bound orbits

TABLE IV. As in Table I, but for neutron resonances in the nucleus ^{48}Ni.

	Gamow		Phase shift	
State	e_α (MeV)	Γ_α (MeV)	e_α (MeV)	Γ_α (MeV)
$2d_{3/2}$	1.099	0.256	1.099	0.273
$1g_{7/2}$	3.397	0.073	3.397	0.073
$1h_{11/2}$	6.513	0.115	6.513	0.115

underestimates the binding energy by about 1 MeV due to the insufficient number of states included in the basis. The HF-BCS-R model agrees very well with the HFB calculation. It is remarkable that, when resonance states are included in the BCS model, the results improve greatly. This is a consequence of the fact that the particle-gas problem is avoided in our BCS formalism.

VI. CONCLUSION

In a description of drip-line nuclei, continuum states play an important role. In the HFB model the quasiparticle continuum is properly taken into account, and one obtains spatially localized matter densities. The traditional BCS approximation of the HFB theory has an important drawback if the full single-particle continuum is taken into account: an unphysical particle gas surrounds the nucleus. Our BCS model with resonances partly overcomes this difficulty.

The standard HFB theory uses a complete system. This basis contains bound and real energy scattering states of a model Hamiltonian. We replaced this basis by the Berggren basis, which contains bound, resonance, and complex energy continuum states. If this basis is truncated (i.e., scattering states with complex energy are neglected) we have a HFB theory based on bound and resonance states. In this approximation the virtual pair scattering occurs between discrete states. The traditional nuclear structure picture can be maintained, since narrow resonances are very similar to bound states.

To simplify the calculation further, we have applied the state-dependent BCS approximation with bound and resonance states. We have shown that the proton drip-line region around the double magic nucleus ^{48}Ni can be very well described by the generalized BCS approach. The absolute binding energies and nuclear radii are in good agreement with the HFB theory. This of course does not mean that the BCS model with resonances always works well. Probably the

TABLE V. As in Table III, but for the $N=22$ isotones.

	^{44}Ti			^{46}Cr			^{48}Fe		
	$-E$	r^2	$-\lambda$	$-E$	r^2	$-\lambda$	$-E$	r^2	$-\lambda$
HFB	376.28	3.51	4.62	383.20	3.58	3.15	387.54	3.65	1.95
HF-BCS-B	374.93	3.50	4.68	382.28	3.57	3.39	383.88	3.64	2.30
HF-BCS-R1	375.49	3.51	4.72	382.45	3.58	3.41	387.02	3.64	2.27
HF-BCS-R2	375.53	3.51	4.74	382.50	3.58	3.41	387.06	3.64	2.25
HF-BCS-R3	375.78	3.51	4.83	382.80	3.58	3.43	387.58	3.65	2.13
HF-BCS-R4	376.20	3.51	4.97	383.32	3.59	3.46	387.68	3.65	2.12

structure of the continuum determines the applicability of the BCS description.

It would be very interesting to make HFB calculation on a truncated Berggren basis (bound and resonance states) but without the BCS approximation. With this type of calculation, one should clearly distinguish between the effect of the background continuum and the effect of the resonance states.

ACKNOWLEDGMENTS

We thank J. Dobaczewski for interesting discussions and for providing us with spherical HF-BCS results. This research was supported in part by the PAI-P3-043 of the Belgian Office for Scientific Policy, and Hungarian OTKA Grant Nos. T029003 and T026244.

[1] K. Bennaceur, J. Dobaczewski, and M. Ploszajczak, Phys. Rev. C **60**, 034308 (1999).
[2] J. Dobaczewski, H. Flocard, and J. Treiner, Nucl. Phys. **A422**, 103 (1984).
[3] J. Dobaczewski, W. Nazarewicz, T. R. Werner, J. F. Berger, C. R. Chinn, and J. Dechargé, Phys. Rev. C **53**, 2809 (1996).
[4] W. Nazarewicz, J. Dobaczewski, T. R. Werner, J. A. Maruhn, and P.-G. Reinhard, Phys. Rev. C **53**, 740 (1996).
[5] J. Terasaki, P.-H. Heenen, P. Bonche, J. Dobaczewski, and H. Flocard, Nucl. Phys. **A593**, 1 (1995).
[6] P. Bonche, S. Levit, and D. Vautherin, Nucl. Phys. **A427**, 278 (1984).
[7] P. Bonche, S. Levit, and D. Vautherin, Nucl. Phys. **A436**, 265 (1985).
[8] N. Sandulescu, R. J. Liotta, and R. Wyss, Phys. Lett. B **394**, 6 (1996).
[9] N. Sandulescu, Nguyen Van Giai, and R. J. Liotta, Phys. Rev. C **61**, 061301 (2000).
[10] Y. K. Ho, Phys. Rep. **99**, 1 (1993).
[11] N. Moiseyev, Phys. Rep. **302**, 211 (1998).
[12] A. T. Kruppa, P.-H. Heenen, H. Flocard, and R. J. Liotta, Phys. Rev. Lett. **79**, 2217 (1997).
[13] M. N. Medikeri and M. K. Mishra, Chem. Phys. Lett. **246**, 26 (1995); M. Bently, Phys. Rev. A **42**, 3826 (1990).
[14] J. Dobaczewski, I. Hamamoto, W. Nazarewicz, and J. A. Sheikh, Phys. Rev. Lett. **72**, 981 (1994).
[15] B. Gyarmati and T. Vertse, Nucl. Phys. **A160**, 523 (1971).
[16] T. Berggren, Nucl. Phys. **A109**, 265 (1968).
[17] R. J. Liotta, E. Maglione, N. Sandulescu, and T. Vertse, Phys. Lett. B **367**, 1 (1996).
[18] P. Ring and P. Schuck, *The Nuclear Many-Body Problem* (Springer-Verlag, Berlin, 1980).
[19] B. Gall, P. Bonche, J. Dobaczewski, H. Flocard, and P.-H. Heenen, Z. Phys. A **348**, 183 (1994).
[20] P. Curutchet, T. Vertse, and R. J. Liotta, Phys. Rev. C **39**, 1020 (1989).
[21] S. Fortunato, A. Insolia, R. J. Liotta, and T. Vertse, Phys. Rev. C **54**, 3279 (1996).
[22] P. Lind, R. J. Liotta, E. Maglione, and T. Vertse, Z. Phys. A **347**, 231 (1994).
[23] T. Vertse, P. Curutchet, and R. J. Liotta, Phys. Rev. C **42**, 2605 (1990).
[24] T. Vertse, R. J. Liotta, and E. Maglione, Nucl. Phys. **A584**, 13 (1995).
[25] T. Vertse, K. F. Pal, and Z. Balogh, Comput. Phys. Commun. **27**, 309 (1982).
[26] E. Chabanat, P. Bonche, P. Haensel, J. Meyer, and R. Schaeffer, Nucl. Phys. **A635**, 231 (1998).
[27] J. Dobaczewski, W. Nazarewicz, and T. R. Werner, Phys. Scr. **T56**, 15 (1995).
[28] P. Möller, J. R. Nix, W. R. Myers, and W. J. Swiatecki, At. Data Nucl. Data Tables **59**, 185 (1995).
[29] Y. Aboussir, J. M. Pearson, A. K. Dutta, and F. Tondeur, Nucl. Phys. **A549**, 155 (1992).
[30] J. Dobaczewski (private communication).
[31] T. Vertse, A. T. Kruppa, R. J. Liotta, W. Nazarewicz, N. Sandulescu, and T. R. Werner, Phys. Rev. C **57**, 3089 (1998).
[32] B. Gyarmati, F. Krisztinkovics, and T. Vertse, Phys. Lett. **41B**, 110 (1972).